International Journal of Food Microbiology 319 (2020) 108494

Contents lists available at ScienceDirect

International Journal of Food Microbiology

journal homepage: www.elsevier.com/locate/ijfoodmicro

Elucidating antimicrobial mechanism of nisin and grape seed extract against *Listeria monocytogenes* in broth and on shrimp through NMR-based metabolomics approach

Xue Zhao[a,c], Lin Chen[a,c], Ji'en Wu[b], Yun He[a,c], Hongshun Yang[a,c,*]

[a] Department of Food Science & Technology, National University of Singapore, Singapore 117542, Singapore
[b] Setsco Services Pte Ltd., 18 Teban Gardens Crescent, Singapore 608925, Singapore
[c] National University of Singapore (Suzhou) Research Institute, 377 Lin Quan Street, Suzhou Industrial Park, Suzhou, Jiangsu 215123, PR China

ARTICLE INFO

Keywords:
Nisin
Plant extract
Omics
Foodborne pathogens
Antimicrobial mechanism
Seafood

ABSTRACT

Nisin and grape seed extract (GSE) have been widely used as food preservatives; however, the mechanism against pathogens at molecular level has not been well elucidated. This work aimed to investigate their antimicrobial effect against *Listeria monocytogenes* and to elucidate the mechanism by NMR-based metabolomics. Nisin exhibited enhanced *in vitro* antilisterial effect when combined with GSE (4.49 log CFU/mL reduction). Marked change in cell membrane permeability was observed in the combination group using confocal laser scanning microscopy; this was verified by increased leakage of protein and nucleic acid. The underlying antimicrobial mechanism was revealed by NMR coupled with multivariate analysis. Significant decreases in threonine, cysteine, ATP, NADP, adenine were observed, whereas a few of metabolites such as lactic acid and γ-aminobutyric acid (GABA) increased after nisin-GSE treatment ($P < 0.05$). Pathway analysis further manifested that the nisin-GSE inhibited the survival of *L. monocytogenes* by blocking the TCA cycle, amino acid biosynthesis and energy-producing pathway. Lastly, nisin and GSE were applied to shrimp and binary combination showed remarkably antilisterial activity (1.79 log CFU/g reduction). GABA shunt and protein degradation from shrimp compensated the unbalanced glycolysis and amino acid metabolism by providing energy and carbon source for *L. monocytogenes* inoculated on shrimp. Thus, they were more tolerant to nisin and GSE stresses as compared to the broth-grown culture.

1. Introduction

Listeria monocytogenes is a pathogenic bacterium which can cause severe foodborne illness or even death particularly in those immunecompromised individuals (Afari and Hung, 2018). Seafood, either raw or processed, has been reported as a major vehicle of *L. monocytogenes* contamination. It is of significant concern as it can survive and multiply in quite stressful environments, such as acidic pH, low temperature, and high salt conditions (Gao and Liu, 2014). Moreover, the high adaptive ability to physicochemical interventions make it challengeable for eradiation of *L. monocytogenes* (Jiang et al., 2011; Vongkamjan et al., 2017). Therefore, a promising strategy is needed to reduce contamination of *L. monocytogenes* in seafood products.

Nisin is a natural cationic and hydrophobic peptide that produced by specific strains of *Lactococcus lactis* (Modugno et al., 2019). As the most widely applied bacteriocin, it has been certified as a generally recognised as safe (GRAS) additive by Food and Drug Administration. It exhibits remarkably antimicrobial activity toward a wide range of Gram-positive bacteria such as *L. monocytogenes* but shows limited effect against Gram-negative bacteria (Campion et al., 2017). Moreover, its effectiveness, solubility and stability is often affected by environmental factors such as pH, temperature, composition, structure, and natural microbiota of food. Thus, the combined use with other antimicrobial agents for food preservation has been proposed as an alternative to increase its action effectiveness (Ibarra-Sánchez et al., 2018).

Grape seed extract (GSE) is by-product of wine and grape industry and is also regarded as a GRAS food additive. It contains substantial bioactive compounds such as proanthocyanidins, epicatechin, catechin, and gallic acid. In recent years, GSE has gained great popularity and attention due to its abundant source, superior health beneficial function and antioxidant ability (Chen et al., 2018; Zhao et al., 2019c) Moreover, GSE shows promising antimicrobial property against many foodborne pathogens such as *L. monocytogenes*, *Staphylococcus aureus*, *Bacillus subtilis*, *Escherichia coli* O157:H7 and *Bacillus cereus* (Perumalla and

* Corresponding author at: Department of Food Science and Technology, National University of Singapore, Singapore 117542, Singapore.
E-mail address: fstynghs@nus.edu.sg (H. Yang).

https://doi.org/10.1016/j.ijfoodmicro.2019.108494
Received 16 August 2019; Received in revised form 10 December 2019; Accepted 19 December 2019
Available online 26 December 2019
0168-1605/ © 2019 Published by Elsevier B.V.

Hettiarachchy, 2011; Sheng et al., 2016).

Metabolomics serves as a systematic approach that provides a "snapshot" of the comprehensive metabolic profiles of biological samples. As an emerging metaboomics technique, nuclear magnetic resonance (NMR) is rapid, non-dustructive, reproducible in revealing the metabolic profiling of microorganisms (Chen et al., 2020b). For instance, NMR has been applied to investigate the metabolic changes that occured in *E. coli* and *L. innocua* after electrolysed water treatment (Liu et al., 2017, 2018). NMR-based metabolomic analysis of *L. monocytogenes* may be helpful for the understanding of the corresponding bacterial response and the underlying antimicrobial mechanisms of different treatments.

The aim of this study was to investigate the antimicrobial effects against *L. monocytogenes* suspension by nisin, GSE and their combined treatment. Cell membrane integrity analysed by confocal laser scanning microscopy (CLSM) and biomacromolecules (protein and nucleic acid) leakage were conducted to preliminarily elucidate the antimicrobial mechanism of each treatment. NMR-based metabolomics couple with multivariate analysis were further applied to study the metabolic changes and reveal the underlying antimicrobial mechanism of nisin and GSE. Lastly, the bacterial reductions and metabolic alterations that occur in *L. monocytogenes* inoculated on shrimp were evaluated and compared with *L. monocytogenes* grew in TSB.

2. Materials and methods

2.1. Preparation of antimicrobial solutions and bacterial strain

The nisin stock solution (2.5% balance sodium chloride, Sigma-Aldrich Chemical Co. St. Singapore) was prepared by dissolving 1 g nisin in 10 mL 0.02 M HCl (10^5 IU/mL). GSE was purchased from Tianjin Jianfeng Natural Product Co., Ltd. (Tianjin, China) and dissolved in sterile DI water using a stirrer. The GSE solution and nisin solution were thoroughly mixed and stirred at room temperature. The antimicrobial solutions were prepared using autoclaved DI water and were subjected to filtration through a sterile syringe filter (0.22 μm) before use.

L. monocytogenes (stereotype 3a, SSA184, isolated from smoked salmon) was provided by Department of Food Science & Technology, National University of Singapore. The strain was activated by culturing in 5 mL Tryptone Soya Broth (TSB, Oxoid, UK) and incubating at 37 °C overnight (Liu et al., 2018). The working suspension of *L. monocytogenes* was prepared by inoculating the activated cultures into 20 mL of fresh TSB (1:100, v/v) and incubating at 37 °C for about 24 h. The cultures with around 9 log colony forming units (CFU)/mL were centrifuged at 5, 000 ×*g* for 10 min at 20 °C and the obtained cell pellets were washed with 0.1 M phosphate-buffered saline (PBS, pH 7.2) twice and resuspended for subsequent analysis (Liu et al., 2018).

2.2. Antimicrobial analysis against L. monocytogenes

In our preliminary study, the inoculated shrimps were treated with nisin or GSE solutions at different concentrations (nisin: 100, 500, 1000, 2000, and 4000 IU/mL; GSE: 0.1%, 0.5%, 1%, and 2%, w/v). The results showed high concentration of GSE (2%, w/v) resulted in undesirable changes on texture or colour qualities of the shrimps. Based on the result that treatment with 1% (w/v) GSE or 2000 IU/mL resulted in the greatest reduction of *L. monocytogenes* without any obvious compromising of the sample qualities. Thus, the working conditions of nisin and GSE were set at 2000 IU/mL and 1%, respectively.

For the *in vitro* antimicrobial test, the *L. monocytogenes* suspension was mixed with nisin (final concentration of 2000 IU/mL), GSE (1%) and their combination, respectively. The suspension treated with sterile DI water was served as the control group. After each treatment, mixed suspension (1 mL) was transferred and immediately neutralised with 9 mL 0.1 M PBS for 5 min to terminate the treatment. The neutralised samples were then decimally diluted and 100 μL of diluent was plated on Tryptone Soya Agar (TSA, Oxoid, UK) plates. The colonies were enumerated after incubating at 37 °C for 48 h and expressed as log CFU/mL. To compare the antimicrobial effect of nisin and GSE against *L. monocytogenes*, the time needed for 1 log CFU/mL reduction was estimated by Weibull model (Chen et al., 2019c).

2.3. Protein leakage and nucleic acid leakage

The protein leakage was tested according to Zhao et al. (2017) with minor modifications. The neutralised suspensions of each treatment collected in Section 2.2 were centrifuged at 8000 ×*g* for 10 min at 24 °C. The supernatant (20 μL) was mixed with 200 μL Coomassie brilliant blue G-250 solution. After incubation at room temperature for 5 min, the absorbance of mixture was read at 595 nm by a fluorescence plate reader (Spectrafluor Plus, Tecan, Durham, NC, USA). Bovine serum albumin (BSA) was used as standard (20–100 μg/mL, $R^2 > 0.99$).

Leakage of nucleic acid was conducted using the method reported by Cui et al. (2018). The supernatant collected was filtered through a microporous membrane (0.22 μm) and diluted for 100 times. Concentration of nucleic acid was expressed as OD_{260} which was measured using a fluorescence plate reader.

2.4. Confocal laser scanning microscopy (CLSM) analysis

Cell membrane permeability and integrity after each treatment was evaluated using an inverted FLUOVIEW® FV 1000 Laser Scanning Confocal Microscope (Olympus, Tokyo, Japan). Two dyes, SYTO®9 and propidium iodide (PI), were equally mixed thoroughly. After staining by 3 μL of mixed dyes in the LIVE/DEAD® BacLight™ Viability Kit L-7007 (Molecular Probes™195, Eugene, USA), 1 mL of treated *L. monocytogenes* was incubated at room temperature in dark for 15 min. Afterwards, 20 μL of *L. monocytogenes* suspension was spread onto glass slides and the fluorescence images were captured immediately (Wang et al., 2019).

2.5. Extraction of L. monocytogenes metabolites

The prepared *L. monocytogenes* pellet was immediately mixed with 1 mL of ice-cold methanol-d_4 (Cambridge Isotope Laboratories, Tewksbury, MA, USA) and frozen in liquid nitrogen (Winder et al., 2008). The mixture was then thawed on ice and further frozen in liquid nitrogen. The freeze-thaw cycles were conducted three times to destroy the membrane structure. The mixture was subsequently extracted at −20 °C overnight, and the metabolic extract was obtained by centrifugation at 12,000 ×*g* for 20 min (4 °C). Trimethylsilylpropanoic acid (TSP, dissolved in methanol-d_4, 10 mM) was mixed with the collected extract as an internal reference at a final concentration of 1 mM. The obtained supernatant (600 μL) was transferred into a 5 mm magnetic tube (Sigma-Aldrich, St. Louis, MO, USA) and immediately subject to NMR analysis.

2.6. NMR analysis of L. monocytogenes metabolic profiles

The prepared samples were tested using a Bruker DRX-500 NMR spectrometer (Bruker, Rheinstetten, Germany) with a frequency of 500.23 MHz via a Triple Inverse Gradient probe (probe temperature: 25 °C). The standard Bruker NOESY pulse sequence (noesypr1d) was applied to obtain the ^{1}H spectrum of each sample and the data were collected with an acquisition time of 3.3 s. Moreover, the spectrum was obtained using 128 scans, and 4 dummy scans, and the relaxation delay was set at 2 s. An automatic pulse calculation experiment (pulsecal) in TopSpin 3.6.0 (Bruker) was applied to modify the 90° pulse length of each result. Furthermore, the free induction decays were multiplied by an exponential function equivalent to a 1-Hz line-broadening factor

before Fourier transformation. For the subsequent identification of metabolic chemicals, the 2D $^{1}H-^{13}C$ heteronuclear single quantum coherence spectroscopy (HSQC) of *L. monocytogenes* samples was acquired using the Bruker hsqcedetgpsisp2.3 pulse sequence at 25 °C. The ^{1}H spectra with a width of 10.0 ppm and the ^{13}C spectra with a width of 180.0 ppm were tested in the F2 and F1 channels, respectively (Zhao et al., 2019a).

Spectral processing and analysis, including the baseline and phase distortions of the resulting spectra were manually corrected using the software TopSpin 3.6.0 (Bruker). Metabolic identification was conducted using 1D ^{1}H and 2D $^{1}H-^{13}C$ spectra cooperatively. The chemical shifts were verified using the Madison Metabolomics Consortium Database (http://mmcd.nmrfam.wisc.edu), the Biological Magnetic Resonance Data Bank (http://www.bmrb.wisc.edu/metabolomics), the Human Metabolome Database (http://www.hmdb.ca/), and related references. Furthermore, the methanol (3.28–3.33 ppm) region was excluded from the spectra and the processed spectra (0.5–10.0 ppm) were normalised to the sum intensities using the software Mestrenova (Mestreab Research SL, Santiago de Compostela, Spain). The normalised ^{1}H spectra were integrated over a series of 0.02 ppm integral width and the obtained binned data were subject to multivariate analysis (Mahmud et al., 2015). The obtained NMR data were further evaluated by principle component analysis (PCA) for group separation and orthogonal projection to latent structures-discriminant analysis (OPLS-DA) to identify the differences between four treatments. Lastly, the variable importance in projection (VIP) was determined and those metabolites with a VIP value > 1 were regarded as the most influential variants in the OPLS models (Chen et al., 2019a).

PCA of the bucket tables was conducted using SIMCA software (version 13.0, Umetrics, Umeå, Sweden). The fold change (FC) of the identified metabolites and related *P* value in pairwise groups were calculated based on the binned data and a volcano plot was constructed. Metabolites with a FC > 2 and $P < 0.05$ were considered as statistically significant (Mahmud et al., 2015). The Euclidean distances between the variables were determined using MatLabR2013b (MathWork, Natick, MA, USA) (Chen et al., 2020a). The enrichment pathway analysis and biological interpretations were performed using MetaboAnalyst 4.0 (http://www.metaboanalyst.ca/) with the screened metabolites and the Kyoto Encyclopedia of Genes and Genomes (KEGG) database (https://www.genome.jp/kegg/pathway.html), respectively.

2.7. Antimicrobial analysis on shrimp

Commercial shrimp (*Litopenaeus vannamei*) was obtained from a local supermarket in Singapore. After removing the head and peel, the samples were autoclaved (15 min, 121 °C) and cooled down before use. For general liquid culture propagation, overnight *L. monocytogenes* cultures (18 h, 37 °C, 200 rpm) were grown in TSB, diluted 1:100 in fresh TSB, and working cultures were grown to mid-exponential phase growth (OD_{600nm} = 0.5–0.8). These cultures were then diluted to an OD_{600nm} = 0.01 for inoculation onto autoclaved shrimps. Subsequently, one autoclaved shrimp (8.0 ± 0.8 g) was spot-inoculated with 80 μL diluted *L. monocytogenes* suspension. Following growth at 25 °C for 24 h, *L. monocytogenes* on shrimp reached a final concentration of around 8 log CFU/g (Dupre et al., 2019). Under sterile conditions the inoculated shrimps were randomly separated into four groups: control (DI water), nisin (2000 IU/mL), GSE (1%, w/v) and combination. The *in vivo* inactivation test was conducted by direct immersing the samples into the antimicrobial solutions. The shrimp collected at different time points (0, 4, 8, 12, 16 and 20 min) was transferred to a sterile stomacher bag containing 72 mL of peptone water (0.1%) for 3-min homogenisation (Masticator Stomacher, IUL Instruments, Germany). For CFU enumeration, decimal dilution by peptone water was conducted and 100 μL of diluent was plated on TSA plates. The colonies were enumerated after incubating at 37 °C for 48 h and expressed as log CFU/g sample (Chen et al., 2019c).

For metabolic analysis of each group, 400 g shrimps were used for *L. monocytogenes* inoculation. After treating the shrimps with nisin and/or GSE for 20 min, the antimicrobial solutions were collected immediately and centrifuged at low speed (500 ×*g*) for 1 min to precipitate debris. The cells were harvested by centrifugation at 12,000 ×*g* for 10 min and then washed with 0.1 M PBS (pH 7.2) for twice (Dupre et al., 2019). Metabolites extraction and NMR testing were conducted under the same conditions as described in Sections 2.5 and 2.6, respectively.

2.8. Statistical analysis

Data were statistically analysed by analysis of variance (ANOVA) of at least in triplicates, independently. Means were compared using the least significant difference (LSD) method with computer software IBM SPSS Statistics Version 23 (International Business Machines Co. Armonk, NY, USA) to assess the effects of different treatments on fillets. Differences with $P < 0.05$ were regarded significant.

3. Results and discussion

3.1. In vitro antimicrobial effect of nisin and GSE on L. monocytogenes

The *in vitro* inactivation effect on *L. monocytogenes* after treatments of nisin and GSE alone and in combination is shown in Fig. 1A. The reduction of *L. monocytogenes* counts reached 0.63–2.88 log CFU/mL when bacterial suspensions were treated with nisin and GSE alone. The killing effect was more marked when combined nisin with GSE, resulting in a significantly increased reduction by up to 2.96 log CFU/mL ($P < 0.05$). The highest bacterial reduction (4.49 log CFU/mL) was observed after exposure to combined nisin and GSE for 10 min.

Moreover, the Weibull model provides the information of the antimicrobial effect by calculating the time needed for 1 log reduction. It took shorter time to reach 1 log reduction for combination treatment (0.21 min) than separate treatment of nisin (0.68 min) or GSE (2.78 min). These results indicated an enhanced inactivation effect when used in combination than separate. Previous reports have confirmed the synergetic antimicrobial effect of combined nisin and other plant-derived antimicrobials. For example, combination of nisin with rosemary essential oil or thyme oil resulted in greater *L. monocytogenes* reduction (Raeisi et al., 2016).

3.2. Protein leakage and nucleic acid leakage of L. monocytogenes

To further evaluate the membrane damage of *L. monocytogenes* caused by different treatments, protein and nucleic acid leakages were determined. The more cytoplasmic protein leaks, the greater the conformation of outer membrane of *L. monocytogenes* cells changes (Chen et al., 2019c). As presented in Fig. 1B, protein leakage of *L. monocytogenes* after different treatments were significantly increased ($P < 0.05$), indicating that the all treatments destroyed the structure of cell membrane to varying degrees. As compared to the control group, protein leakage leakage of *L. monocytogenes* treated with GSE increased to 5.24 μg/mL. Higher protein leakage was observed when the *L. monocytogenes* was treated with nisin and GSE-nisin, which reached 9.42 and 11.31 μg/mL, respectively.

The leakage of nucleic acid at 260 nm was detected as shown in Fig. 1C. In the control group, no nucleic acid was be detected, indicating that the cell membrane was under normal condition (Sun et al., 2018). Similar to the results of extracellular protein analysis, the absorbance values of nisin and nisin-GSE groups were significantly higher than that of the control group ($P < 0.05$). It suggested that the cell membrane was severely destroyed after the action of nisin, resulting in the following leakage of nucleic acid. The higher level of protein and nucleic acid leakages by treatments of nisin and GSE-nisin indicated that nisin was more effective in the irreversible disruption of cell membrane as compared to GSE. It is well supported by a previous

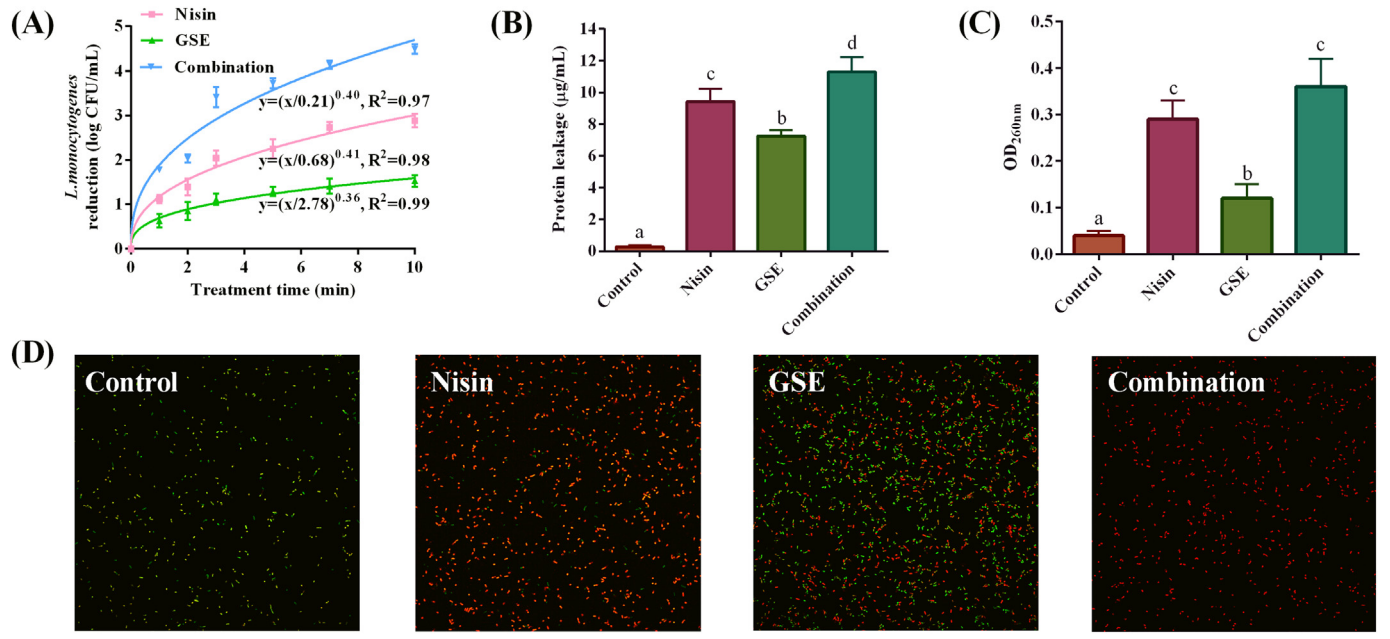

Fig. 1. *In vitro* antimicrobial test. *L. monocytogenes* reduction (A), protein leakage (B), nucleic acid leakage (C) and confocal laser scanning microscopy images of *L. monocytogenes* cells under different treatments (D). Note: Different lowercase letters indicate that values are significantly different ($P < 0.05$).

research which stated the pore formation ability of nisin in bacterial cell membranes (Adhikari et al., 2012).

3.3. Changes in membrane permeability assessed using CLSM

To observe the membrane permeability and overall integrity of *L. monocytogenes* under different treatments, CLSM was conducted and the results are shown in Fig. 1D. According to staining principle, both live and dead cells can be stained with SYTO9 and emit green fluorescence, while dead bacteria can be stained with PI and emit red fluorescence. Additionally, the bacterial cells shown in yellow colour are regarded as injured cells (Panda et al., 2018).

As shown in CLSM images, the *L. monocytogenes* cells in control group emitted bright green fluorescence with very limited yellow or red colour, indicating that majority of the cells were still alive. After treatment with GSE, the ratio of cells in yellow fluorescence increased to 73.11% due to the increased permeability of cell membranes while death damage was at kept at a relatively low level. For the *L. monocytogenes* cells treated with nisin, the ratio of dead cells increased to 52.12% while the injured cells made up of 9.25% of total counts, indicating the cell membrane of nisin-treated cells was disrupted. These results suggested that the antimicrobial effect of nisin against *L. monocytogenes* may be more disruptive and deadly than that of GSE. Moreover, the result suggested that nisin played a more important role in the membrane damage of *L. monocytogenes* than GSE. Previous studies have reported that the mechanism of action of nisin was to increase permeability of microbial cell membranes, resulting in pore generation and cell collapse (Santos et al., 2018). Furthermore, the proportion of cells after treatment with combined nisin and GSE labelled with red fluorescence increased to 91.02%, while green fluorescence was almost invisible. The results demonstrated that most of the cell membranes of *L. monocytogenes* were markedly damaged after combined treatment, leading to apoptosis of cells (Wang et al., 2019). The sublethal or lethal injury caused by nisin and GSE could be attributed to impaired DNA and protein syntheses or enzyme activities (Lourenço et al., 2017).

3.4. Metabolic profiles of L. monocytogenes in TSB

Representative ^{1}H NMR spectra (0–10 ppm) of *L. monocytogenes* under nisin and GSE treatments and assignment of most abundant signals are shown in Fig. 2A. Identification of metabolites in *L. monocytogenes* was conducted using a combination of 1D ^{1}H and 2D ^{1}H−^{13}C NMR results, metabolic database and related references. In total, 45 metabolites were unambiguous assigned and the corresponding chemical shifts are shown in Table S1. Generally, the metabolome of *L. monocytogenes* was composed of amino acids, sugars, organic acids, alcohols, nucleotides, and some other primary or secondary metabolites.

In the high field region (0.5–3.0 ppm) of the analysed spectra of *L. monocytogenes* extracts, the major signals belonged to amino acids (leucine, valine, isoleucine, etc.) and organic acids (acetic acid, lactic acid, pyruvic acid, etc.) (Liu et al., 2018). Ethanol, acetoin, and putrescine were also assigned in this region. In the middle field region (3.0–5.5 ppm) the α-protons of some amino acids (proline, glycine, etc.) contribute to the observed spectra. Sugars (α-D-glucose, β-D-glucose, etc.) and sugar phosphates (glucose-1-phosphate, glucose-6-phosphate, etc.) were also recorded with strong peaks in this region. Furthermore, most signals in the low field region of spectra are assigned to nucleobases (uracil and adenine), nucleosides (uridine and adenosine), and nucleotides (ATP, ADP, AMP, etc.). The results were in accordance with a previous study which investigated and profiled a relative complete metabolome of *L. monocytogenes* grown at different temperatures (Singh et al., 2011). Furthermore, all these identified metabolites of *L. monocytogenes* were observed among different treatment groups with varying peak intensities.

Among all metabolites, 36 of them with no overlapping chemical shifts were further analysed for relative quantification. To preliminarily visualise the changes in these metabolite levels due to treatment of nisin and GSE, a heat map was plotted in a blue-pink colour scale using the z-score transformed NMR data (Fig. 2B). The blue colour indicates an increase while the pink colour represents a decrease in metabolite level as compared to the control group. The levels of most amino acids such as leucine, valine and cysteine declined whereas a few of them like γ-aminobutyric acid (GABA) increased after nisin and GSE treatments. For most of the identified nucleotide-related compounds such as ATP, AMP and adenosine, lower levels were observed under nisin and GSE treatments. These results were in accordance with previous studies that suggested the blocked energy supply and amino acid biosynthesis by

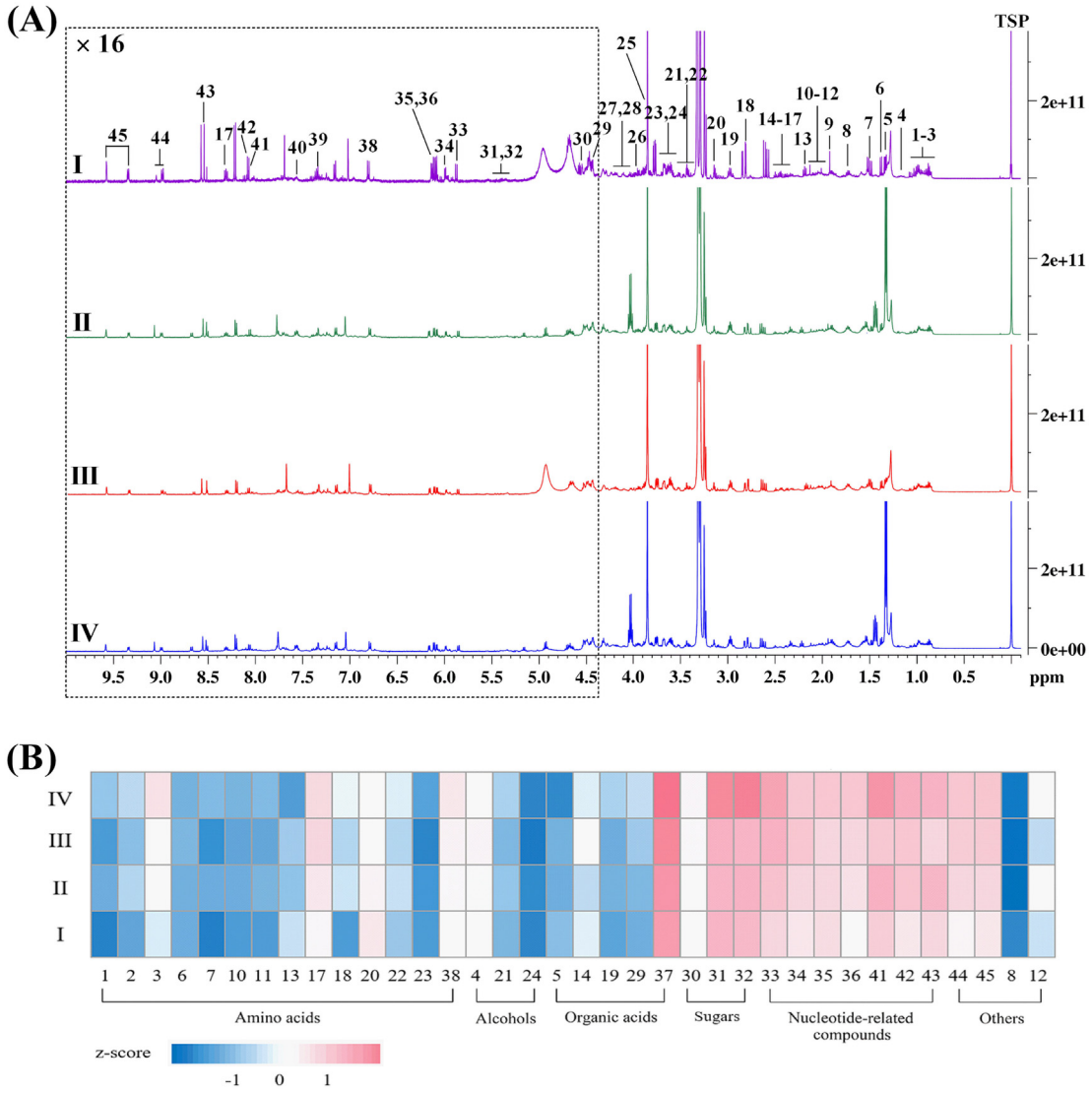

Fig. 2. Representative ^{1}H NMR spectra of *L. monocytogenes* cells under different treatments (A); heatmap of identified metabolites (B). Note: group I–IV, *L. monocytogenes* under deionised (DI) water, grape seed extract (GSE), nisin, and combination treatments, respectively. (For interpretation of the references to colour in this figure, the reader is referred to the web version of this article.)

nisin and some phenolic compounds (Kołodziejczyk et al., 2013; Pernin et al., 2019).

3.5. Metabolic changes of *L. monocytogenes* in TSB

To further analyse the metabolites in different groups, targeted profiling by PCA was conducted (Chen et al., 2019a). The model quality parameters (Fig. 3A) results being R^2X = 0.993 and Q^2 = 0.986, indicated that model had good interpretative and predictable abilities. The PCA score plot (Fig. 3B) shows well clustering of samples from the same group and distinctive separations between different treatments. Clear discrimination indicated that different treatments resulted in the significant metabolic changes among groups. The control and nisin groups were negatively influenced by PC1 and PC2, respectively, while GSE and nisin-GSE groups were positively affected by PC1 (Tables S2, S3). The longest inter-group distance among four groups was observed between the control group and nisin-GSE group, suggesting that the combination treatment resulted in the largest changes in metabolites of *L. monocytogenes*. Moreover, the clustering of GSE and nisin-GSE groups indicated that the GSE contributed more to the metabolic changes as compared to nisin.

As the score plot provided the grouping information between different groups, the loading plot indicated discriminative metabolites that contributed to the separations of variables. As shown in Fig. 3C, most of the metabolites such as lactic acid, oxoglutaric acid, cysteine, threonine, γ-aminobutyric acid and leucine had large loading on PC1 while PC2 was characterised by a few metabolites such as glutamine, pyruvic acid, and 2,3-butanediol. These metabolites may be marker metabolites that responded to different treatments.

The above-mentioned PCA results provided a global overview of the metabolic response of *L. monocytogenes* following nisin and GSE treatments. Furthermore, a more supervised model, OPLS-DA was applied to examine separations between three pairwise groups: the control and GSE groups (I–II), the control and nisin groups (I–III), and the control and combination groups (I–IV). The established OPLS-DA models presented good prediction ability and interpreted the data well, based on the corresponding R^2 and Q^2 values. Moreover, the score plots of three OPLS-DA models (Fig. 4A1–C1) demonstrated clear separation between control group and three antimicrobial-treated groups. The results indicated that the effects of nisin and GSE were detectable in the metabolome of *L. monocytogenes*.

OPLS-DA loading S-line (Fig. 4A2–C2) was performed to determine

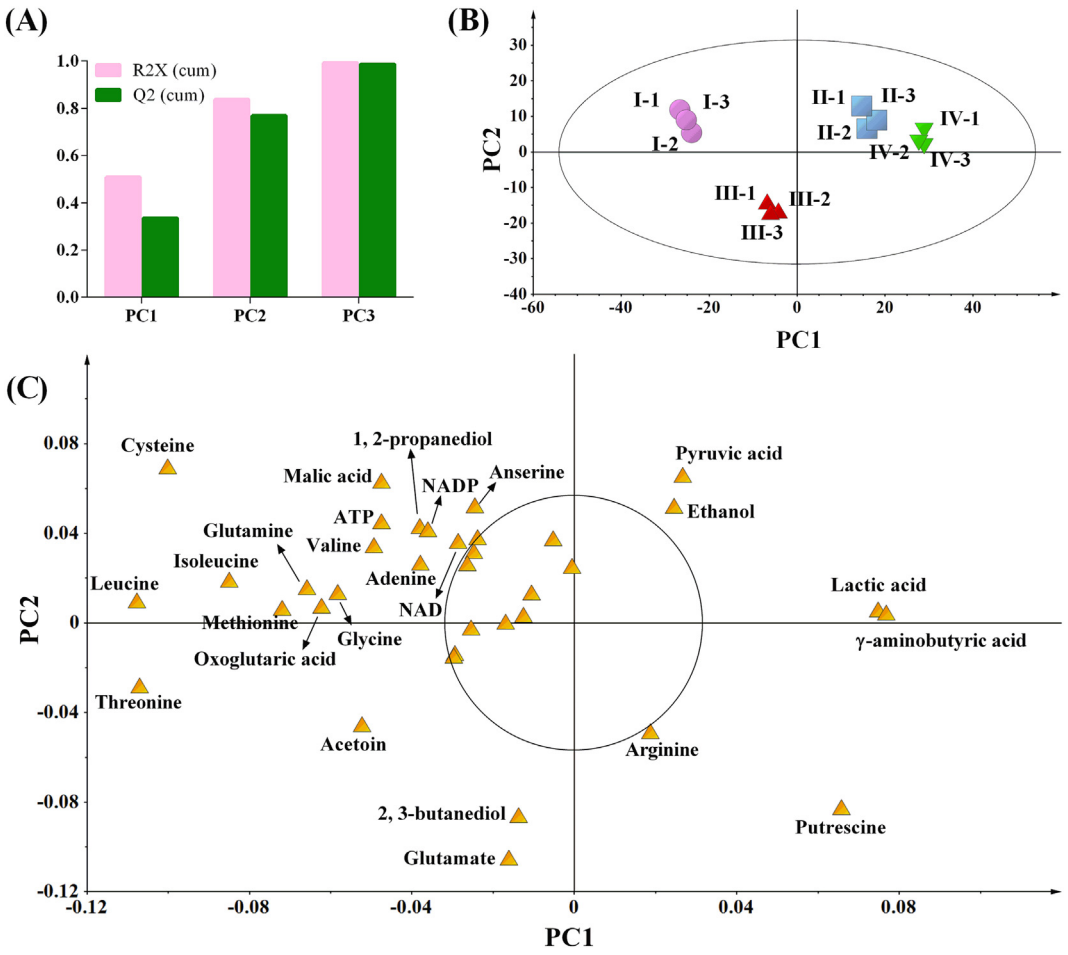

Fig. 3. Principal component analysis (PCA) for the metabolite profile of *L. monocytogenes*. The principal components explaining variances used in PCA (A); PCA score plot (B); PCA loading plot (C). Note: group I–IV, *L. monocytogenes* under of deionised (DI) water, grape seed extract (GSE), nisin, and combination treatments, respectively.

the major metabolites which contributed to the pairwise differentiations (Chen et al., 2019b). Potential discriminative metabolites were identified from the corresponding loading S-line plots. As compared to the control group, a distinct increase in lactic acid and putrescine and an obvious decrease in leucine, isoleucine, glutamate, acetoin, etc. were observed in GSE group (Fig. 4A2). The S-line of I–III (Fig. 4B2) indicated that the nisin treatment was associated with increased contents of γ-aminobutyric acid and glutamine as well as depleted levels of isoleucine, threonine, malic acid, etc. As shown in Fig. 4C2, the combined treatment was associated with higher levels of lactic, pyruvic and γ-aminobutyric acids and marked reduce of ATP, NADP, malic acid, oxoglutaric acid, and some amino acids.

Moreover, the metabolites with a VIP value > 1 were chosen as candidates for inter-group separation (Park et al., 2019). As for the combination group, more discriminating variables were selected for pair-wise separation in I–IV (15 metabolites with VIP > 1) as compared to I–II and I–III comparisons, indicating that more disturbed metabolism was induced by the combination treatment. Thus, we primarily focused on the effect of combined nisin and GSE on *L. monocytogenes* metabolism in following analysis.

An enhanced volcano plot coupled with VIP and correlation coefficient, as shown in Fig. 5A, provides an all-scaled and straightforward way to study differential metabolites. In total, 18 metabolites showed over 2-FC ($P < 0.05$) and 9 of these greatly altered metabolites showed top 20% VIP value (VIP ≥ 1.017). The results from enhanced volcano plots are consistent with the corresponding coefficient loading plots where metabolites with major difference between groups appear in hot colours. It is worth noticing that the altered metabolites due to combined treatment are primarily distributed in the top left region of the volcano plot, indicating that combined nisin and GSE stimulation mainly led to declined metabolite contents in *L. monocytogenes*. Following the combination stimulation, the *L. monocytogenes* extracts in the treated group are highlighted with significant increases (2.1–2.4 times as compared to the control group) of lactic acid and γ-aminobutyric acid, along with reductions of metabolites including cysteine, ATP, leucine, isoleucine, fumaric acid, malic acid and threonine. These metabolites are potential sublethal markers due to combined nisin and GSE stimulation.

3.6. Alternative metabolic pathways of *L. monocytogenes* in TSB

Pathway analysis was performed to identify the related pathway that was caused by the combined nisin and GSE treatment based on the chosen candidates and database. In total, 22 pathways were predicted and 8 of them with $P < 0.05$ were regarded as significant metabolic pathways that involved in the antimicrobial process (Table S4). The selected pathways were alanine, aspartate and glutamate metabolism; aminoacyl-tRNA biosynthesis; valine, leucine and isoleucine biosynthesis; cysteine and methionine metabolism; glutathione metabolism; butanoate metabolism; citrate cycle (TCA cycle); and pyruvate metabolism (Fig. 5B).

Based on the KEGG pathway database, the disturbance in metabolic status and relevant metabolic pathways of *L. monocytogenes* under binary treatment of nisin and GSE are summarised and presented in

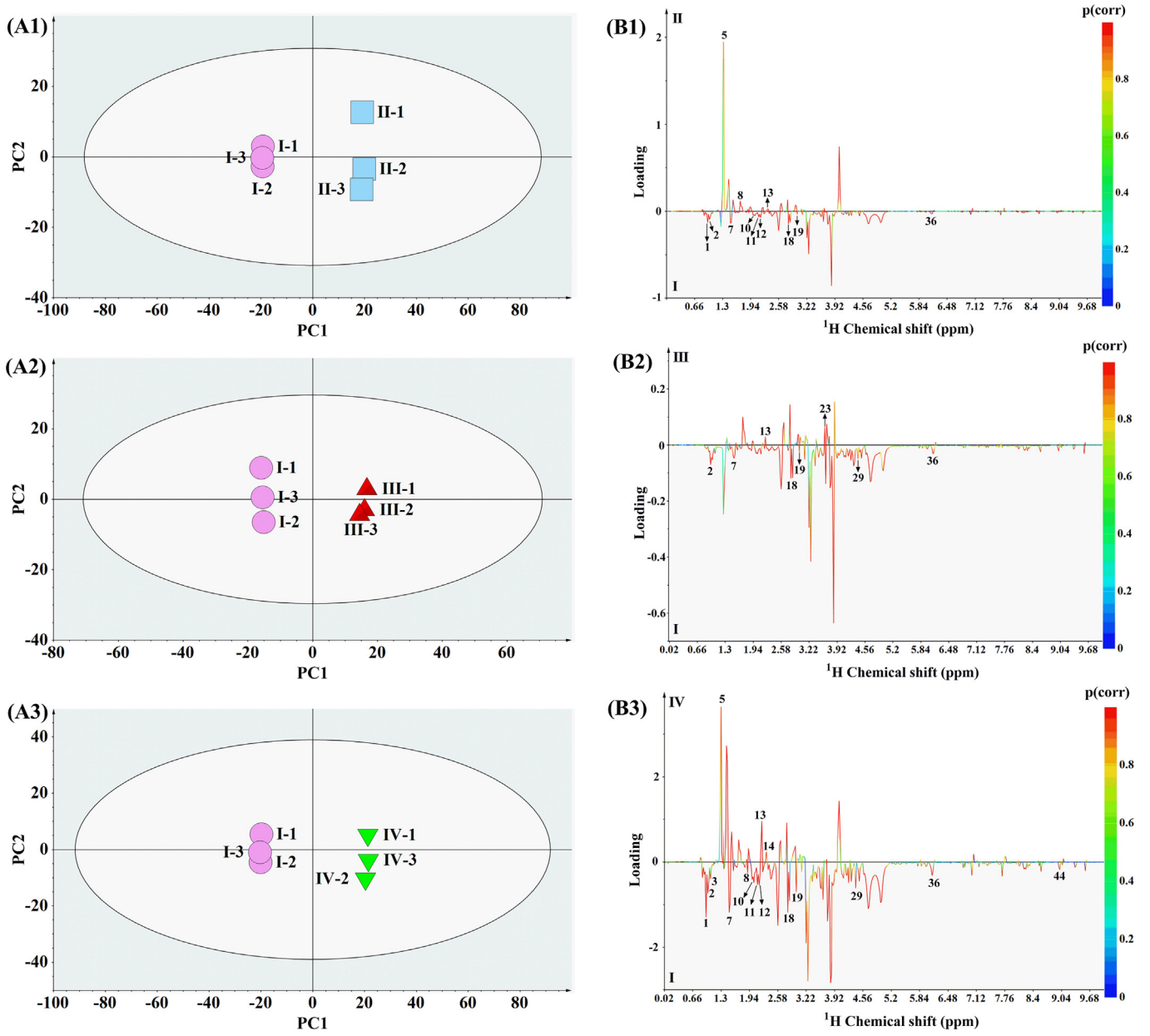

Fig. 4. Orthogonal partial least squares discriminant analysis (OPLS-DA) comparison results of pairwise groups. OPLS-DA score plot (A1) and loading S-line plot (B1) of groups I–II, R^2 = 0.88, Q^2 = 0.99; OPLS-DA score plot (A2) and loading S-line plot (B2) of groups I–III, R^2 = 0.89, Q^2 = 0.99; OPLS-DA score plot (A3) and loading S-line plot (B3) of groups I–IV, R^2 = 0.94, Q^2 = 0.99; Note: group I–IV, *L. monocytogenes* under deionised (DI) water, grape seed extract (GSE), nisin, and combination treatments, respectively.

Fig. 5C. Metabolites in green or red colour represent that their contents were higher or lower in the combination group in comparison with the control group, respectively. Amino acid metabolism was found to be the most influenced pathway under combined nisin and GSE treatment. Lower concentrations of amino acids (e.g. leucine, isoleucine, alanine, cysteine, and methionine) were observed. The amino acid biosynthesis was perturbed under nisin and GSE stimulations; this could be explained as the amino acid biosynthesis is very sensitive toward hostile environment, such as oxidation, heat, or acid stress (Jozefczuk et al., 2010). It is also possible that nisin and GSE caused osmotic stress as some amino acids such as glutamate and glycine play important role in sustaining the cytoplasmic osmolality and preventing the breakdown of subcellular structures (Maria-Rosario et al., 1995). The weakened biosynthesis of amino acids could further affect the *L. monocytogenes* growth by inhibiting protein synthesis (Cui et al., 2018). These results were in accordance with previous work. The authors indicated that the antimicrobial effect of blueberry extract (sharing a similar composition as GSE used in our study) was a combined effect of various phenolic substances and these compounds work collectively in blocking TCA cycle and hindering protein biosynthesis (Sun et al., 2018).

Amino acid metabolism can provide carbon skeletons entering the TCA pathway. TCA cycle is not only the major way to generate energy but also the most common pathway for complete oxidation of sugar, lipid and protein inside the cell (Sun et al., 2018). In our study, malic acid and oxoglutaric acid, the major intermediates of the TCA cycle, were significantly depleted after the nisin and GSE treatment ($P < 0.05$), while the content of fumarate and succinic acid was slightly reduced. These results suggested that the TCA cycle was impaired and weakened. The blocked TCA cycle would result in weakened cellular respiration and inadequate energy supply, finally causing death of bacteria (Kołodziejczyk et al., 2013; Pernin et al., 2019). Simultaneously, it is also noted that γ-aminobutyric acid increased significantly

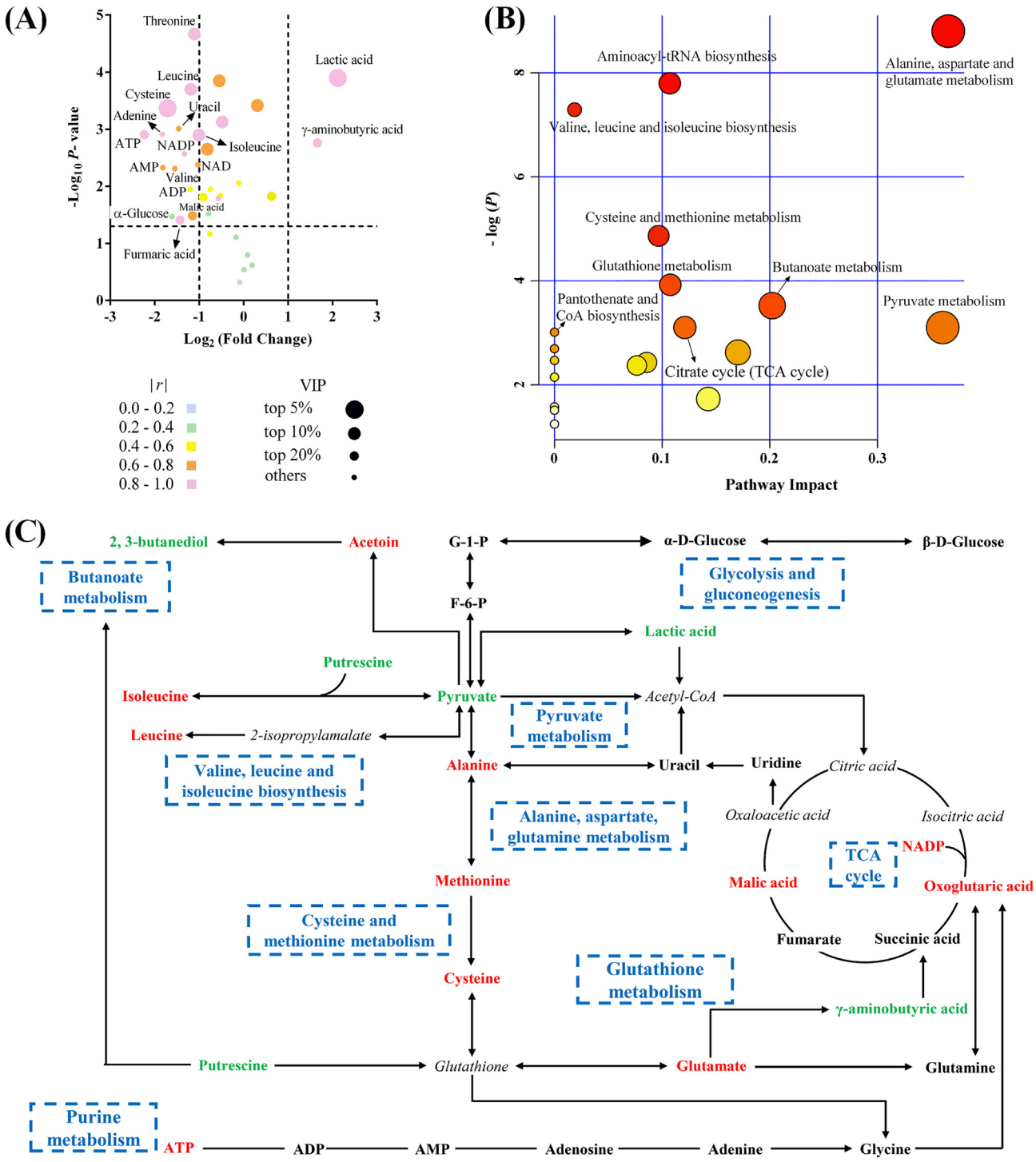

Fig. 5. An enhanced volcano plot of screened *L. monocytogenes* metabolites in control (I) and combination group (IV); overview of pathway analysis of groups I and IV (B); metabolic pathway of *L. monocytogenes* in broth altered by stress of combined nisin and GSE (C). Note: group I and group IV represent *L. monocytogenes* inoculated in broth under deionised (DI) water treatment and combination treatments, respectively; metabolites coloured in green or red represent significantly higher or lower concentration in group IV as compared to I, respectively ($P < 0.05$); metabolites in italic were not detected or while metabolites in bold black did not change significantly ($P > 0.05$). (For interpretation of the references to colour in this figure legend, the reader is referred to the web version of this article.)

after treatment with nisin and GSE. Indeed, this metabolite is obtained by glutamate decarboxylation and it plays quite an important role in survival and adaptation to different stresses (Braschi et al., 2018). The elevated level of γ-aminobutyric acid would be helpful in compensating the weakened TCA cycle by further converting to succinic acid (Feehily et al., 2013).

The biosynthesis of amino acids is also related to the energy transduction and energy metabolism of *L. monocytogenes* as some amino acids (e.g. glutamine and glutamate) are able to provide ATP by substrate-level phosphorylation (Drake et al., 2012). The decrease in ATP level is often reflected at the transcriptional level, being one of the most remarkable responses to diverse external stress. Slightly lower adenine and adenosine levels were recorded. It is possibly due to the weakening of the nucleotide metabolism, resulting in diminished ability to

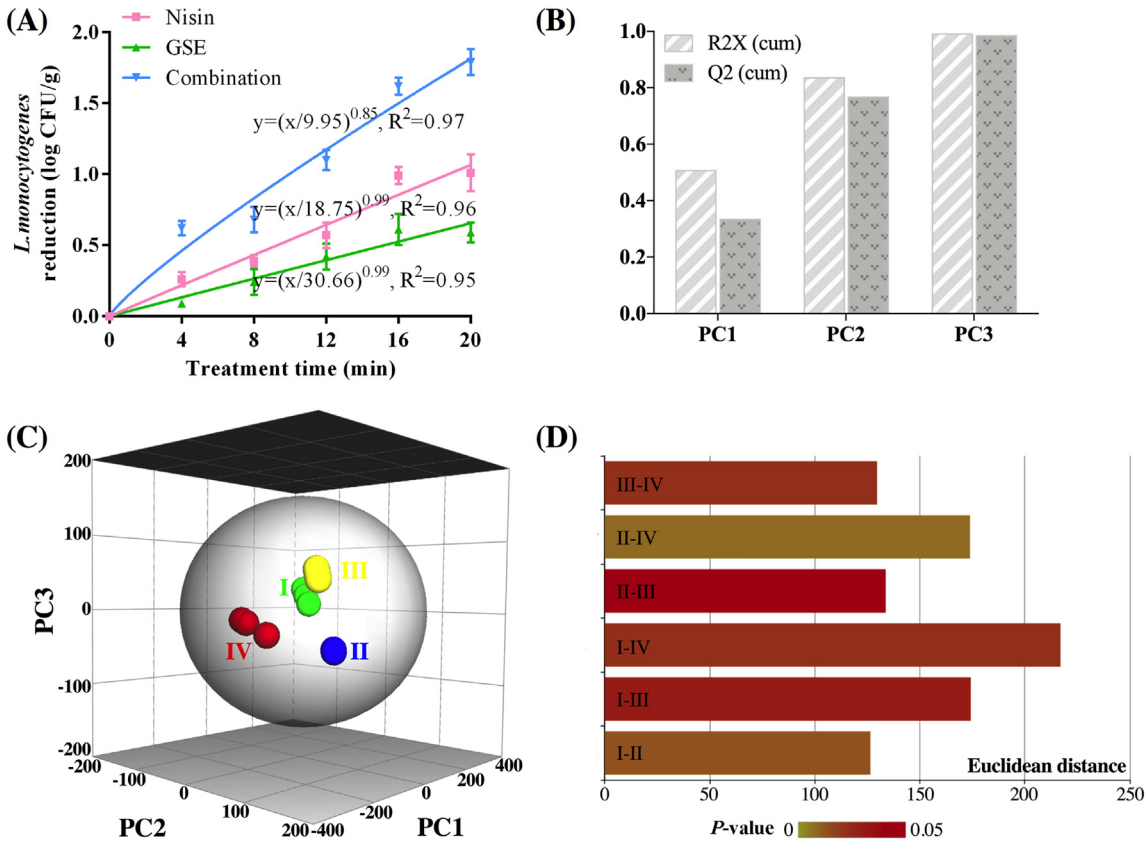

Fig. 6. Antimicrobial effect of nisin, GSE and their combination against *L. monocytogenes* inoculated on shrimp (A); principal component analysis (PCA) for the metabolite profile of *L. monocytogenes* inoculated on shrimp: the principal components explaining variances (B); 3D PCA score plot (C); Euclidean distances between each group (D). Note: group I–IV, *L. monocytogenes* under of deionised (DI) water, nisin, grape seed extract (GSE), and combination treatments, respectively.

synthesise DNA and RNA (Lourenço et al., 2017). Moreover, the catabolic disruption in energy-producing pathway results in an insufficient acetoin production; this was in accordance with our result that the acetoin level was significantly lower in the combination group ($P < 0.05$) (Stasiewicz et al., 2011).

3.7. Antimicrobial effect against L. monocytogenes inoculated on shrimp

In this study, shrimp was selected as a representative high-risk seafood for *L. monocytogenes* contamination (Elbashir et al., 2018). The antimicrobial effects of nisin and GSE alone or in combination against *L. monocytogenes* inoculated on autoclaved shrimp are shown in Fig. 6A. The application of nisin resulted in a reduction of 1.01 log CFU/g of *L. monocytogenes* on autoclaved shrimp. The *in vivo* anti-listerial effect of nisin is dependent on food matrix especially the fatty acid composition as well as surface hydrophobicity (Lourenço et al., 2017). Within the same treatment time, GSE showed a slightly lower antimicrobial effect (0.59 log CFU/g reduction). A previous report showed that GSE at 1.25 mg/mL reduced *L. monocytogenes* population (~2 log CFU/g reduction) on tomato surfaces after treatment for 2 min (Bisha et al., 2010). The antimicrobial effectiveness of GSE against *L. monocytogenes* on different foods is related to the food and GSE composition, treatment time and concentration of GSE (Su and D'Souza, 2013).

Similar to the results of the *in vitro* inactivation test, *L. monocytogenes* inoculated on shrimp was more sensitive to combined treatment (1.79 CFU/g reduction). Weibull fitting further verified this conclusion. It showed that the combination group required 9.95 min to reduce 1 log CFU/g reduction of *L. monocytogenes*, which was significantly shorter than that of nisin-treated (18.75 min) or GSE-treated (30.66 min) groups ($P < 0.05$). On the other hand, the antimicrobial effect of nisin and GSE against *L. monocytogenes* inoculated on shrimp was less than that against bacterial suspension. This might be due to the complex components in food matrices which react with the antimicrobial agents and impair their antilisterial ability (Chen et al., 2019c).

3.8. Alternative metabolic pathways of L. monocytogenes on shrimp

Moreover, beneath the reduction surface, nisin and GSE induced metabolic changes in *L. monocytogenes* inoculated on shrimp were analysed. The metabolic profiles of *L. monocytogenes* inoculated on autoclaved shrimps were obtained, showing high metabolic similarity to the bacteria cells in TSB.

To better understand the *in vivo* effect of nisin and GSE on *L. monocytogenes*, PCA analysis of *L. monocytogenes* from shrimp samples was performed. The first three principal components almost explained of the whole dataset (PC1: 65.9%, PC2: 19.5% and PC3: 14.0%) and the high Q^2 value (0.99) suggested an excellent predictive quality of the constructed PCA model (Fig. 6B) (Chen et al., 2020a).

The metabolome-based separation is shown in the PCA score plot (Fig. 6C). It is observed that the nisin and/or GSE treated samples were clearly separated from the control group. The Euclidean distances of pairwise variables were determined based on the PCA score plot (Fig. 6D). The Euclidean distances between different treatment groups in this study ranged from 126.54 to 217.04. It is noteworthy that the longest Euclidean distance was observed between the control group (I) and the combination group (IV), suggesting their greatest metabolic differences.

Based on the aforementioned PCA results, OPLS-DA model was further developed for selected pairwise comparison, I vs IV. The built model shows quite good reliability, as guaranteed by high R^2 (0.98) and Q^2 (0.99) values (data was not shown). According to the extracted

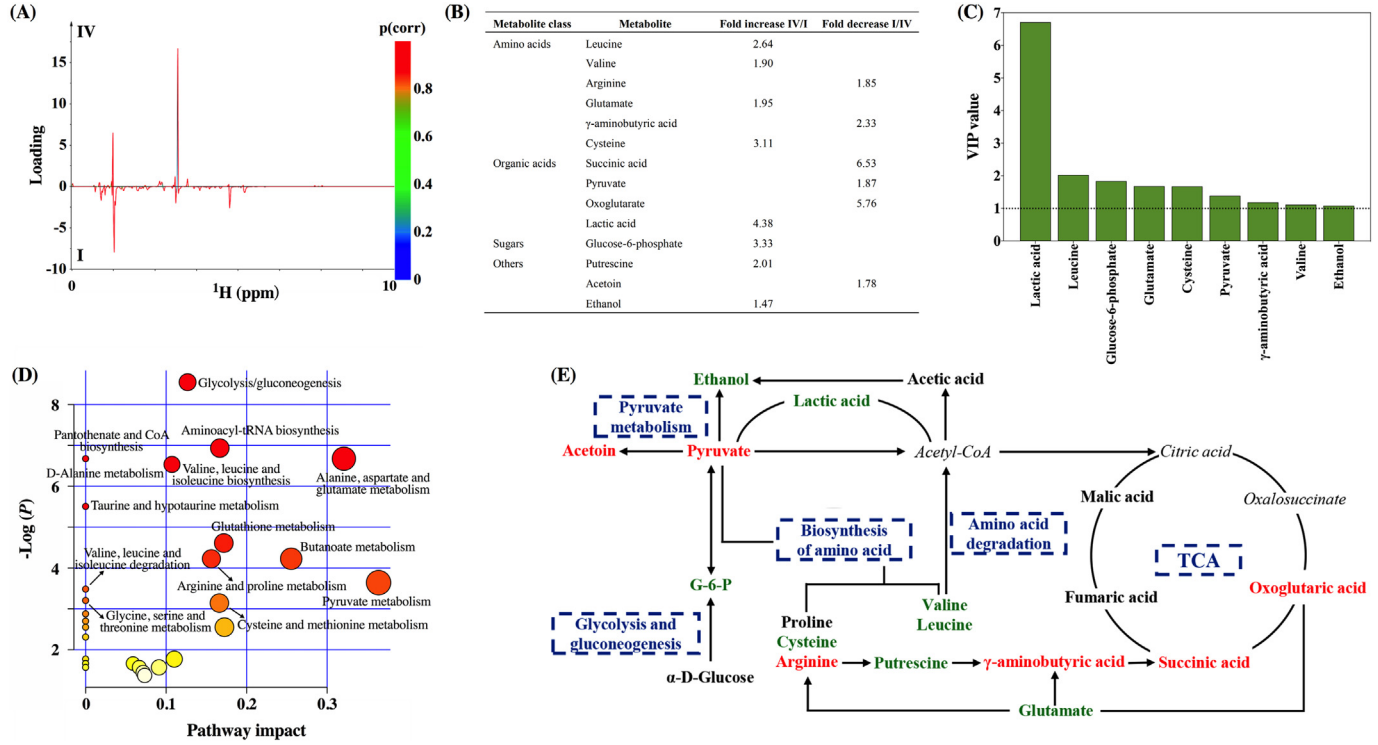

Metabolite class	Metabolite	Fold increase IV/I	Fold decrease I/IV
Amino acids	Leucine	2.64	
	Valine	1.90	
	Arginine		1.85
	Glutamate	1.95	
	γ-aminobutyric acid		2.33
	Cysteine	3.11	
Organic acids	Succinic acid		6.53
	Pyruvate		1.87
	Oxoglutarate		5.76
	Lactic acid	4.38	
Sugars	Glucose-6-phosphate	3.33	
Others	Putrescine	2.01	
	Acetoin		1.78
	Ethanol	1.47	

Fig. 7. Orthogonal partial least squares discriminant analysis (OPLS-DA) loading S-line plot of I–IV, $R^2 = 0.98$, $Q^2 = 0.99$ (A); fold change of metabolites with significant difference ($P < 0.05$) (B); screened metabolites with VIP score > 1 (C); overview of the pathway analysis of I–IV (D); metabolic pathway of *L. monocytogenes* inoculated on shrimp altered by combined nisin and GSE treatment (E). Note: group I and group IV represent *L. monocytogenes* inoculated on shrimp under deionised (DI) water and combination treatments, respectively; metabolites coloured in green or red represent significantly higher or lower concentration in group IV as compared to I, respectively ($P < 0.05$); metabolites in italic were not detected while metabolites in bold black did not change significantly ($P > 0.05$). (For interpretation of the references to colour in this figure legend, the reader is referred to the web version of this article.)

loading S-line plot (Fig. 7A), most of the identified metabolites showed downward tendencies. Also, the red colour of most of the peaks implied significant metabolic differences between group I and group IV. These findings collectively indicated that nisin combined with GSE significantly decreased the concentration of a large variety of metabolites in *L. monocytogenes* inoculated on shrimp ($P < 0.05$).

For the comparisons of the metabolite concentrations, the samples were subject to fold-changes analysis (Fig. 7B). Among all identified metabolites, 25 of them were down-regulated after combined treatment and 6 of them were decreased significantly (FC: 1.78–6.53, $P < 0.05$). Moreover, metabolites such as glutamate, ethanol, lactic acid, glucose-6-phosphate, and putrescine were significantly up-regulated as compared to those in group I (FC: 1.47–4.38, $P < 0.05$).

The vital metabolites that contributed to the discrimination between group I and group II were identified, VIP scores were further calculated (Fig. 7C). The results revealed that 9 metabolites (lactic acid, leucine, glucose-6-phosphate, glutamate, pyruvate, etc.) with VIP value > 1 were possible biomarkers for the characterisation of nisin + GSE response to *L. monocytogenes* on shrimp. Based on these selected candidates, pathway analysis was carried out. As shown in Fig. 7D and Table S5, 13 pathways (Glycolysis/gluconeogenesis; aminoacyl-tRNA biosynthesis; pantothenate and CoA biosynthesis; alanine, aspartate and glutamate metabolism; valine, leucine and isoleucine biosynthesis; taurine and hypotaurine metabolism; glutathione metabolism; arginine and proline metabolism; butanoate metabolism; pyruvate metabolism; valine, leucine and isoleucine degradation; glycine, serine and threonine metabolism; cysteine and methionine metabolism) with P value < 0.05 were identified as most affected metabolic pathways when treating shrimp-based *L. monocytogenes* with nisin and GSE.

The assumptive biochemical pathways of *L. monocytogenes* after combined treatment are proposed and shown in Fig. 7E. Glycolysis was found to be the most affected biochemical pathway after combined treatment of nisin and GSE. In this study, lower concentration of pyruvate and higher concentration of glucose-6-phosophate indicated unbalanced glycolysis of *L. monocytogenes* under combined treatment. The hypothesis is consistent with a previous study showing that some glycolysis-related genes in *L. monocytogenes* were underexpressed such as *pgm* while others like *pdhD* were overexpressed after exposure to sublethal stresses of natural essential oils (i.e., carvacrol essential oil) (Braschi et al., 2018). Moreover, the elevated level of ethanol and lactic acid (end-product of glucose fermentation) implied a possible metabolic switch from oxidation to fermentation which could be served as shunt for sustaining glycolysis (Nilsson et al., 2013). In addition, the reduced acetoin production revealed that the metabolic flux of *L. monocytogenes* was disrupted. This was suggested in a previous study that reduced acetoin production could be regarded as an indicator of growth and metabolic suppression of *L. monocytogenes* (Romick and Fleming, 1998).

Metabolism through the GABA shunt is an important nitrogen source for bacteria. Arginine is one of the nitrogen sources for *L. monocytogenes* (Schneider et al., 2002). Conversion of arginine to putrescine via glutamate in this study suggested an initiation of GABA shunt pathway. The obtained GABA from putrescine and glutamate can be further metabolised to succinic acid to maintain the incomplete TCA cycle of *L. monocytogenes* (Le Lay et al., 2015). Moreover, the GABA obtained by the decarboxylation of glutamate, can be metabolised and converted to succinate. However, the lower levels of succinic acid *L. monocytogenes* inoculated on shrimp might indicate that the GABA shunt in response to combined treatment of nisin and GSE could only partially compensate the induced disturbance in TCA cycle. Amino acid metabolism is also a primary target during different stresses. In this study, an obvious increase of valine, cysteine, glutamate and leucine in *L. monocytogenes* inoculated on shrimp were observed after combined treatment. These amino acids play important roles in sustaining the stabilisation of cellular osmolarity (Zhao et al., 2019b). Thus, their

elevation might be an implication that the bacterial cells inoculated on shrimp were struggled to survive and resist in response to the combined stress.

Overall, these results show that the metabolic response to nisin and GSE stresses were dissimilar between *L. monocytogenes* grew in TSB and cells inoculated on shrimp, based on the overall profiles of metabolic network. The difference in metabolic response could be related with the composition of culture media. As compared to the simple composition of TSB (tryptone, soytone, glucose, sodium chloride and dipotassium phosphate), shrimp is composed of abundant nutrient substances especially protein. It is possible that shrimp proteins degraded to amino acids by *L. monocytogenes* proteases. In line with the notion that *L. monocytogenes* utilised amino acids from shrimp as energy and carbon sources, four amino acids as mentioned before were present in higher contents in the *L. monocytogenes* bacteria inoculated on shrimp as compared to the broth cultures. The results were similar to a previous study that compared the metabolomics of *S. aureus* inoculated on chicken breast or in Luria broth (Dupre et al., 2019).

On the other hand, hypothetically the metabolic alterations in *L. monocytogenes* cells was related to the acidic environment provided by the combined nisin and GSE solution whose pH value was around 4. The cells inoculated on shrimp (pH: 6.3, slightly acidic) was acid-adapted; thus it displayed enhanced tolerant to extracellular pH changes caused by nisin and GSE as compared to the TSB (pH: 7.3) cultures (Skandamis et al., 2012).

Lastly, it is known that nisin effectiveness is generally lower in complex food matrices than in laboratory growth media as it can undergo proteolytic degradation or be adsorbed by food biomolecules. As suggested by Gharsallaoui et al. (2016), when nisin is in contact with food matrices, the antimicrobial activity of nisin heavily depends on the food characteristics. The application of nisin in meat and seafood matrices is greatly affected by the glutathione, a molecule capable of inactivating nisin activity by glutathione S-transferase (Stergiou et al., 2006).

4. Conclusion

This research studied the antimicrobial effect and mechanism of nisin and GSE against *L. monocytogenes*. In conclusion, nisin combined with GSE yielded an enhanced antimicrobial effect against *L. monocytogenes*, which was more effective than working alone. The antimicrobial mechanism of binary treatment is possibly a combination of cell membrane breakdown by nisin and disturbance in the intracellular metabolism of *L. monocytogenes* mainly caused by GSE. The cell structure was damaged and the permeability of cell membrane of *L. monocytogenes* was changed after an initial effect of nisin; this was confirmed by the leakage of biomacromolecules (protein and nucleic acid). NMR-based metabolomics further revealed that a more lasting effect by combined nisin and GSE, which blocked some vital metabolic pathways such as TCA cycle, energy metabolism and amino acid biosynthesis. The *in vivo* application suggested that the combination of nisin and GSE still provides satisfactory efficiency for reducing *L. monocytogenes* contamination on shrimp. Due to the interaction between shrimp matrix and nisin, as well as the high protein concentration and slightly acidic condition of shrimp, the metabolic response of *L. monocytogenes* inoculated on shrimp was quite different. GABA shunt and protein degradation from shrimp collectively compensated the unbalanced glycolysis and altered amino acid metabolism in *L. monocytogenes* inoculated on shrimp, leading to an enhanced resistant to the combined treatment. Overall, the study shows the effectiveness of NMR-based metabolomics to elucidate the antimicrobial mechanism of nisin and GSE on *L. monocytogenes* with different growth conditions, providing guidance for seafood industry to control *L. monocytogenes* contamination.

Declaration of competing interest

We declare that we do not have any commercial or associative interest that represents a conflict of interest in connection with this manuscript. We have no financial and personal relationships with other people or organizations that can inappropriately influence our work.

Acknowledgements

The work was funded by Singapore Ministry of Education Academic Research Fund Tier 1 (R-143-000-A40-114), Projects 31371851 and 31471605 supported by NSFC and Natural Science Foundation of Jiangsu Province (BK20181184), and an industry project (R-143-000-A21-597) from Shanghai ProfLeader Biotech Co., Ltd.

Appendix A. Supplementary data

Supplementary data to this article can be found online at https://doi.org/10.1016/j.ijfoodmicro.2019.108494.

References

Adhikari, M.D., Das, G., Ramesh, A., 2012. Retention of nisin activity at elevated pH in an organic acid complex and gold nanoparticle composite. Chem. Commun. 48 (71), 8928–8930.
Afari, G.K., Hung, Y., 2018. A meta-analysis on the effectiveness of electrolyzed water treatments in reducing foodborne pathogens on different foods. Food Control 93, 150–164.
Bisha, B., Weinsetel, N., Brehm-Stecher, B.F., Mendonca, A., 2010. Antilisterial effects of gravinol-s grape seed extract at low levels in aqueous media and its potential application as a produce wash. J. Food Prot. 73 (2), 266–273.
Braschi, G., Serrazanetti, D.I., Siroli, L., Patrignani, F., De Angelis, M., Lanciotti, R., 2018. Gene expression responses of *Listeria monocytogenes* Scott A exposed to sub-lethal concentrations of natural antimicrobials. Int. J. Food Microbiol. 286, 170–178.
Campion, A., Morrissey, R., Field, D., Cotter, P.D., Hill, C., Ross, R.P., 2017. Use of enhanced nisin derivatives in combination with food-grade oils or citric acid to control *Cronobacter sakazakii* and *Escherichia coli* O157: H7. Food Microbiol. 65, 254–263.
Chen, L., Tan, G.J.T., Pang, X., Yuan, W., Lai, S., Yang, H., 2018. Energy regulated nutritive and antioxidant properties during the germination and sprouting of broccoli sprouts (*Brassica oleracea* var. *italica*). J. Agric. Food Chem. 66 (27), 6975–6985.
Chen, L., Tan, J.T.G., Zhao, X., Yang, D., Yang, H., 2019a. Energy regulated enzyme and non-enzyme-based antioxidant properties of harvested organic mung bean sprouts (*Vigna radiata*). LWT- Food Sci. Technol. 107, 228–235.
Chen, L., Wu, J., Li, Z., Liu, Q., Zhao, X., Yang, H., 2019b. Metabolomic analysis of energy regulated germination and sprouting of organic mung bean (*Vigna radiata*) using NMR spectroscopy. Food Chem. 286, 87–97.
Chen, L., Zhang, H., Liu, Q., Pang, X., Zhao, X., Yang, H., 2019c. Sanitising efficacy of lactic acid combined with low-concentration sodium hypochlorite on *Listeria innocua* in organic broccoli sprouts. Int. J. Food Microbiol. 295, 41–48.
Chen, L., Zhao, X., Wu, J.E., He, Y., Yang, H., 2020a. Metabolic analysis of salicylic acid-induced chilling tolerance of banana using NMR. Food Res. Int. 128, 108796.
Chen, L., Zhao, X., Wu, J.E., Liu, Q., Pang, X., Yang, H., 2020b. Metabolic characterisation of eight *Escherichia coli* strains including “Big Six” and acidic responses of selected strains revealed by NMR spectroscopy. Food Microbiol. 88, 103399.
Cui, H., Zhang, C., Li, C., Lin, L., 2018. Antimicrobial mechanism of clove oil on *Listeria monocytogenes*. Food Control 94, 140–146.
Drake, K.J., Sidorov, V.Y., McGuinness, O.P., Wasserman, D.H., Wikswo, J.P., 2012. Amino acids as metabolic substrates during cardiac ischemia. Exp. Biol. Med. 237 (12), 1369–1378.
Dupre, J.M., Johnson, W.L., Ulanov, A.V., Li, Z., Wilkinson, B.J., Gustafson, J.E., 2019. Transcriptional profiling and metabolomic analysis of Staphylococcus aureus grown on autoclaved chicken breast. Food Microbiol. 82, 46–52.
Elbashir, S., Parveen, S., Schwarz, J., Rippen, T., Jahncke, M., DePaola, A., 2018. Seafood pathogens and information on antimicrobial resistance: a review. Food Microbiol. 70, 85–93.
Feehily, C., O'Byrne, C.P., Karatzas, K.A.G., 2013. Functional γ-aminobutyrate shunt in *Listeria monocytogenes*: role in acid tolerance and succinate biosynthesis. Appl. Environ. Microbiol. 79 (1), 74–80.
Gao, H., Liu, C., 2014. Biochemical and morphological alteration of *Listeria monocytogenes* under environmental stress caused by chloramine-T and sodium hypochlorite. Food Control 46, 455–461.
Gharsallaoui, A., Oulahal, N., Joly, C., Degraeve, P., 2016. Nisin as a food preservative: part 1: physicochemical properties, antimicrobial activity, and main uses. Crit. Rev. Food Sci. Nutr. 56 (8), 1262–1274.
Ibarra-Sánchez, L.A., Van Tassell, M.L., Miller, M.J., 2018. Antimicrobial behavior of phage endolysin PlyP100 and its synergy with nisin to control *Listeria monocytogenes* in Queso Fresco. Food Microbiol. 72, 128–134.
Jiang, Z., Neetoo, H., Chen, H., 2011. Efficacy of freezing, frozen storage and edible antimicrobial coatings used in combination for control of *Listeria monocytogenes* on

roasted turkey stored at chiller temperatures. Food Microbiol. 28 (7), 1394–1401.
Jozefczuk, S., Klie, S., Catchpole, G., Szymanski, J., Cuadros-Inostroza, A., Steinhauser, D., Steinhauser, D., Selbig, J., Willmitzer, L., 2010. Metabolomic and transcriptomic stress response of *Escherichia coli*. Mol. Syst. Biol. 6 (1), 364–380.
Kołodziejczyk, K., Sójka, M., Abadias, M., Viñas, I., Guyot, S., Baron, A., 2013. Polyphenol composition, antioxidant capacity, and antimicrobial activity of the extracts obtained from industrial sour cherry pomace. Ind. Crop. Prod. 51, 279–288.
Le Lay, J., Bahloul, H., Sérino, S., Jobin, M., Schmitt, P., 2015. Reducing activity, glucose metabolism and acid tolerance response of *Bacillus cereus* grown at various pH and oxydo-reduction potential levels. Food Microbiol. 46, 314–321.
Liu, Q., Wu, J.E., Lim, Z.Y., Aggarwal, A., Yang, H., Wang, S., 2017. Evaluation of the metabolic response of *Escherichia coli* to electrolysed water by ^{1}H NMR spectroscopy. LWT- Food Sci. Technol. 79, 428–436.
Liu, Q., Wu, J., Lim, Z.Y., Lai, S., Lee, N., Yang, H., 2018. Metabolite profiling of *Listeria innocua* for unravelling the inactivation mechanism of electrolysed water by nuclear magnetic resonance spectroscopy. Int. J. Food Microbiol. 271, 24–32.
Lourenço, A., Kamnetz, M.B., Gadotti, C., Diez-Gonzalez, F., 2017. Antimicrobial treatments to control *Listeria monocytogenes* in queso fresco. Food Microbiol. 64, 47–55.
Mahmud, I., Kousik, C., Hassell, R., Chowdhury, K., Boroujerdi, A.F., 2015. NMR spectroscopy identifies metabolites translocated from powdery mildew resistant rootstocks to susceptible watermelon scions. J. Agric. Food Chem. 63 (36), 8083–8091.
Maria-Rosario, A., Davidson, I., Debra, M., Verheul, A., Abee, T., Booth, I.R., 1995. The role of peptide metabolism in the growth of *Listeria monocytogenes* ATCC 23074 at high osmolarity. Microbiol 141 (1), 41–49.
Modugno, C., Kmiha, S., Simonin, H., Aouadhi, C., Cañizares, E.D., Lang, E., et al., 2019. High pressure sensitization of heat-resistant and pathogenic foodborne spores to nisin. Food Microbiol. 103244, 1–7.
Nilsson, R.E., Ross, T., Bowman, J.P., Britz, M.L., 2013. MudPIT profiling reveals a link between anaerobic metabolism and the alkaline adaptive response of *Listeria monocytogenes* EGD-e. PLoS One 8 (1), e54157.
Panda, S., Rout, T.K., Prusty, A.D., Ajayan, P.M., Nayak, S., 2018. Electron transfer directed antibacterial properties of graphene oxide on metals. Adv. Mater. 30 (7), 1702149.
Park, S.E., Seo, S.H., Kim, E.J., Byun, S., Na, C.S., Son, H.S., 2019. Changes of microbial community and metabolite in kimchi inoculated with different microbial community starters. Food Chem. 274, 558–565.
Pernin, A., Guillier, L., Dubois-Brissonnet, F., 2019. Inhibitory activity of phenolic acids against *Listeria monocytogenes*: deciphering the mechanisms of action using three different models. Food Microbiol. 80, 18–24.
Perumalla, A.V.S., Hettiarachchy, N.S., 2011. Green tea and grape seed extracts—potential applications in food safety and quality. Food Res. Int. 44 (4), 827–839.
Raeisi, M., Tabaraei, A., Hashemi, M., Behnampour, N., 2016. Effect of sodium alginate coating incorporated with nisin, Cinnamomum zeylanicum, and rosemary essential oils on microbial quality of chicken meat and fate of *Listeria monocytogenes* during refrigeration. Int. J. Food Microbiol. 238, 139–145.
Romick, T.L., Fleming, H.P., 1998. Acetoin production as an indicator of growth and metabolic inhibition of *Listeria monocytogenes*. J. Appl. Microbiol. 84 (1), 18–24.
Santos, J.C.P., Sousa, R.C.S., Otoni, C.G., Moraes, A.R.F., Souza, V.G.L., Medeiros, E.A.A., Espitiad, P.J.P., Piresa, A.C.S., Coimbraa, J.S.R., Soare, N.F.F., 2018. Nisin and other antimicrobial peptides: production, mechanisms of action, and application in active food packaging. Innov. Food Sci. Emerg. Technol. 48, 179–194.
Schneider, B.L., Ruback, S., Kiupakis, A.K., Kasbarian, H., Pybus, C., Reitzer, L., 2002. The *Escherichia coli* gabDTPC operon: specific γ-aminobutyrate catabolism and nonspecific induction. J. Bacteriol. 184 (24), 6976–6986.
Sheng, L., Olsen, S.A., Hu, J., Yue, W., Means, W.J., Zhu, M.J., 2016. Inhibitory effects of grape seed extract on growth, quorum sensing, and virulence factors of CDC "top-six" non-O157 Shiga toxin producing *E. coli*. Int. J. Food Microbiol. 229, 24–32.
Singh, A.K., Ulanov, A.V., Li, Z., Jayaswal, R.K., Wilkinson, B.J., 2011. Metabolomes of the psychrotolerant bacterium *Listeria monocytogenes* 10403S grown at 37 °C and 8 °C. Int. J. Food Microbiol. 148 (2), 107–114.
Skandamis, P.N., Gounadaki, A.S., Geornaras, I., Sofos, J.N., 2012. Adaptive acid tolerance response of *Listeria monocytogenes* strains under planktonic and immobilized growth conditions. Int. J. Food Microbiol. 159 (2), 160–166.
Stasiewicz, M.J., Wiedmann, M., Bergholz, T.M., 2011. The transcriptional response of *Listeria monocytogenes* during adaptation to growth on lactate and diacetate includes synergistic changes that increase fermentative acetoin production. Appl. Environ. Microbiol. 77 (15), 5294–5306.
Stergiou, V.A., Thomas, L.V., Adams, M.R., 2006. Interactions of nisin with glutathione in a model protein system and meat. J. Food Prot. 69 (4), 951–956.
Su, X., D'Souza, D.H., 2013. Grape seed extract for foodborne virus reduction on produce. Food Microbiol. 34 (1), 1–6.
Sun, X., Zhou, T., Wei, C., Lan, W., Zhao, Y., Pan, Y., Wu, V.C.H., 2018. Antibacterial effect and mechanism of anthocyanin rich Chinese wild blueberry extract on various foodborne pathogens. Food Control 94, 155–161.
Vongkamjan, K., Benjakul, S., Vu, H.T.K., Vuddhakul, V., 2017. Longitudinal monitoring of *Listeria monocytogenes* and *Listeria* phages in seafood processing environments in Thailand. Food Microbiol. 66, 11–19.
Wang, Y., Qin, Y., Zhang, Y., Wu, R., Li, P., 2019. Antibacterial mechanism of plantaricin LPL-1, a novel class IIa bacteriocin against *Listeria monocytogenes*. Food Control 97 (17), 87–93.
Winder, C.L., Dunn, W.B., Schuler, S., Broadhurst, D., Jarvis, R., Stephens, G.M., Goodacre, R., 2008. Global metabolic profiling of *Escherichia coli* cultures: an evaluation of methods for quenching and extraction of intracellular metabolites. Anal. Chem. 80 (8), 2939–2948.
Zhao, L., Zhang, Y., Yang, H., 2017. Efficacy of low concentration neutralised electrolysed water and ultrasound combination for inactivating *Escherichia coli* ATCC 25922, *Pichia pastoris* GS115 and *Aureobasidium pullulans* 2012 on stainless steel coupons. Food Control 73, 889–899.
Zhao, X., Wu, J., Chen, L., Yang, H., 2019a. Effect of vacuum impregnated fish gelatin and grape seed extract on metabolite profiles of tilapia (*Oreochromis niloticus*) fillets during storage. Food Chem. 293, 418–428.
Zhao, L., Zhao, X., Wu, J.E., Lou, X., Yang, H., 2019b. Comparison of metabolic response between the planktonic and air-dried *Escherichia coli* to electrolysed water combined with ultrasound by ^{1}H NMR spectroscopy. Food Res. Int. 125, 108607.
Zhao, X., Zhou, Y., Zhao, L., Chen, L., He, Y., Yang, H., 2019c. Vacuum impregnation of fish gelatin combined with grape seed extract inhibits protein oxidation and degradation of chilled tilapia fillets. Food Chem. 294, 316–325.